



OPEN ACCESS

EDITED BY

Sam Vinko,
University of Oxford, United Kingdom

REVIEWED BY

Markus Kuster,
European X-Ray Free Electron Laser,
Germany
Enrico Allaria,
Elettra Sincrotrone Trieste, Italy

*CORRESPONDENCE

Haixiao Deng,
✉ denghx@sari.ac.cn
Bo Liu,
✉ bo.liu@zjlab.org.cn

RECEIVED 23 February 2023

ACCEPTED 12 May 2023

PUBLISHED 25 May 2023

CITATION

Liu T, Huang N, Yang H, Qi Z, Zhang K,
Gao Z, Chen S, Feng C, Zhang W, Luo H,
Fu X, Liu H, Faatz B, Deng H, Liu B, Wang D
and Zhao Z (2023), Status and future of
the soft X-ray free-electron laser
beamline at the SHINE.
Front. Phys. 11:1172368.
doi: 10.3389/fphy.2023.1172368

COPYRIGHT

© 2023 Liu, Huang, Yang, Qi, Zhang, Gao,
Chen, Feng, Zhang, Luo, Fu, Liu, Faatz,
Deng, Liu, Wang and Zhao. This is an
open-access article distributed under the
terms of the [Creative Commons
Attribution License \(CC BY\)](https://creativecommons.org/licenses/by/4.0/). The use,
distribution or reproduction in other
forums is permitted, provided the original
author(s) and the copyright owner(s) are
credited and that the original publication
in this journal is cited, in accordance with
accepted academic practice. No use,
distribution or reproduction is permitted
which does not comply with these terms.

Status and future of the soft X-ray free-electron laser beamline at the SHINE

Tao Liu¹, Nanshun Huang², Hanxiang Yang³, Zheng Qi¹,
Kaiqing Zhang¹, Zhangfeng Gao¹, Si Chen¹, Chao Feng¹,
Wei Zhang¹, Hang Luo¹, Xiaoxi Fu¹, He Liu³, Bart Faatz¹,
Haixiao Deng^{1*}, Bo Liu^{1*}, Dong Wang¹ and Zhentang Zhao¹

¹Shanghai Advanced Research Institute, Chinese Academy of Sciences, Shanghai, China, ²Zhangjiang Lab, Chinese Academy of Sciences, Shanghai, China, ³University of Chinese Academy of Sciences, Beijing, China

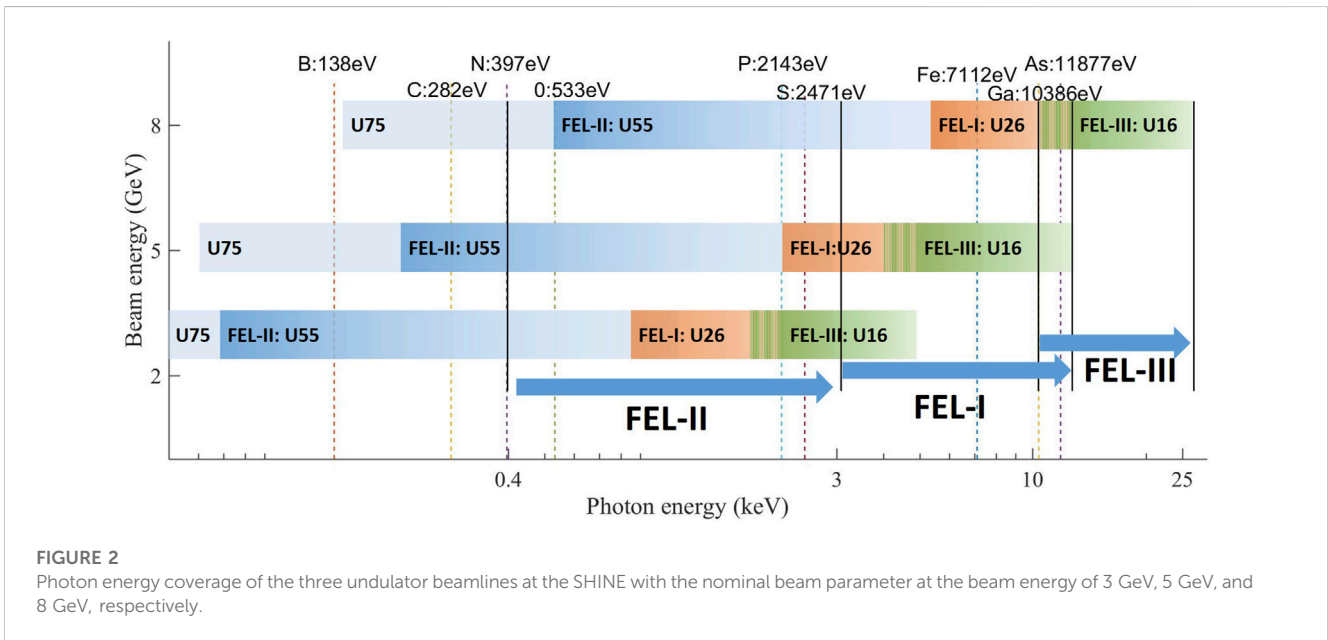
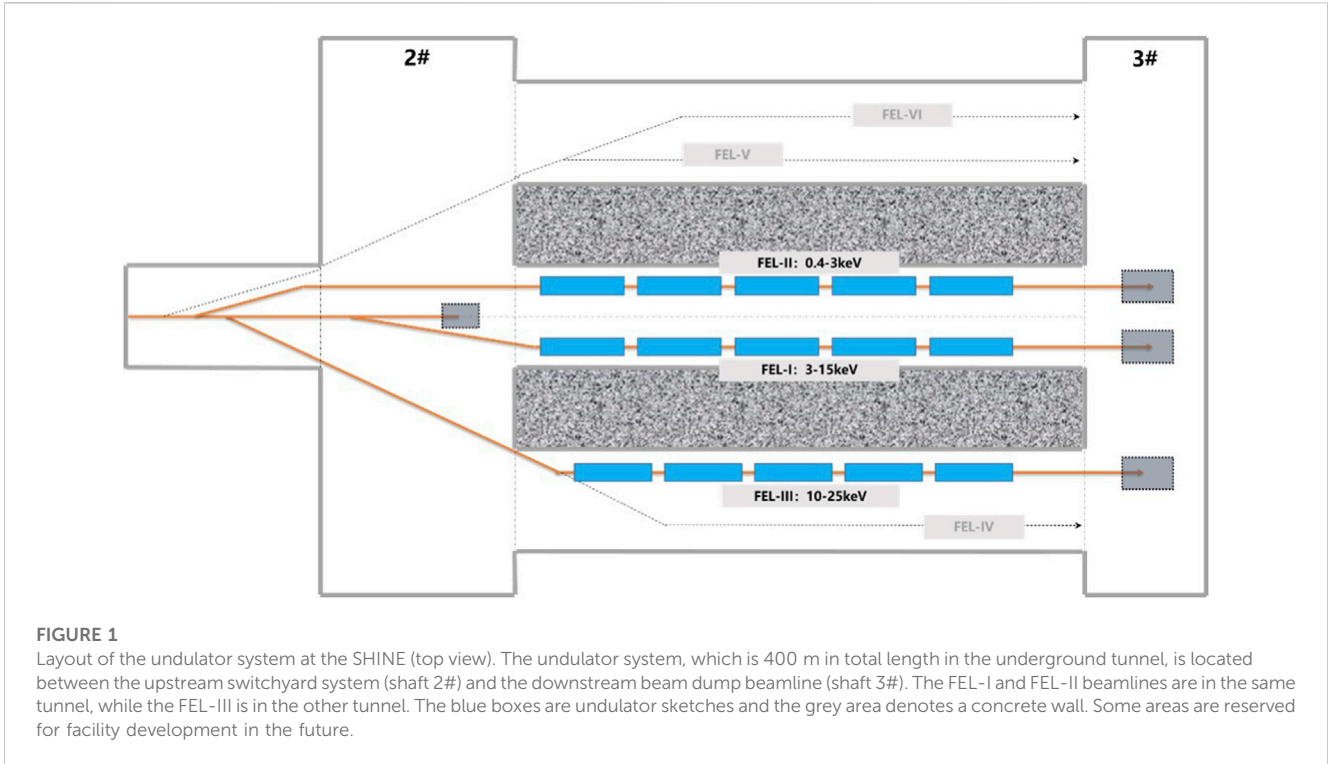
The Shanghai High repetition rate XFEL and Extreme light facility (SHINE) is under construction and aims at generating X-rays between 0.4 and 25 keV with three FEL beamlines at repetition rates of up to 1 MHz. The soft X-ray FEL beamline, FEL-II, will be ready for commissioning in 2025. It is designed to cover the photon energy from 0.4 to 3 keV, in which the baselines of the FEL operation modes are self-amplified spontaneous emission (SASE), self-seeding, echo-enabled harmonic generation (EEHG), and polarization control. Therefore, a high repetition-rate external seed laser, large period length modulator, soft X-ray monochromator, planar undulator, and elliptically polarized undulator have been adopted in the FEL-II beamline. Several potentials such as an ultra-short pulse mode and a multi-color mode are also foreseeable without significant equipment changes in the follow-up operation. A dual-period undulator design is suggested for the echo-enabled harmonic generation (EEHG) commissioning, and it has great potential to break through the unreachable energy of the fully coherent X-ray in the future. The FEL-II beamline will deliver SASE radiation and fully coherent radiation in all the wavelengths of interest.

KEYWORDS

SHINE, FEL, x-ray, SASE, self-seeding, external seeding, harmonic lasing, polarization

1 Introduction

Free-electron lasers (FELs) [1] hold a great capability to generate high intensity, ultra-short, tunable coherent radiation pulses [2, 3], opening up new frontiers of ultra-fast and ultra-small science at atomic length scales [4–6]. High gain FELs have been in operation for users with the great success of several operational facilities around the world, such as FLASH [7], LCLS [8], SACLA [9], FERMI [10], PAL-XFEL [11], European-XFEL ([12]), SwissFEL [13], and SXFEL [14, 15]. The spectral range of these FEL facilities is usually operating in the X-ray regime, which basically chooses self-amplified spontaneous emission (SASE) [16, 17] and external/self-seeding FELs [18–23] as the baseline operation modes. A SASE FEL has the advantages of a simple setup, technological maturity, and excellent transverse coherence, while it typically lacks temporal coherence. External/self-seeding FELs perfectly respond to the problem and provide nearly Fourier-transform limited pulses in the X-ray regime, which mainly includes high-gain harmonic generation (HGHG) [18, 19, 24], echo-enabled harmonic generation (EEHG) [20, 21, 25–30], and soft and hard X-ray self-seedings [22,



23, 31–36]. To further extend the FEL output performance and increase the flexibility of FEL facilities, more advanced FEL modes, such as cascading seeding, the fresh bunch technique, and polarization control have been demonstrated in FEL facilities and supported FEL user experiments.

The Shanghai High repetition rate XFEL and Extreme light facility, abbreviated as SHINE, aims to join the exclusive XFEL club as one of the most advanced user facilities by delivering femtosecond X-ray pulses with up to one million pulses per second. The SHINE is

designed to deliver photons between 0.4 keV and 25 keV at a repetition rate as high as 1 MHz using a superconducting linear accelerator (LINAC) [37]. It consists of an 8 GeV CW superconducting RF Linac, 3 undulator beamlines, 3 X-ray beamlines, and 10 experimental stations in phase-I, and started its construction in April 2018. In this article, we briefly describe the three undulator beamline scheme designs shown in Figure 1, and mainly focus on the soft X-ray FEL beamline, i.e., FEL-II with several advanced FEL operation modes and a flexible schematic design.

In front of the undulator beamlines at the SHINE, the nominal electron beam properties are as follows: the maximum electron beam energy is 8 GeV, the peak current is approximately 1500 A with a bunch charge of 100 pC, the normalized transverse emittance is 0.4–0.5 mm-mrad, the sliced energy spread is approximately 0.01%, and the maximum repetition rate is up to 1 MHz. For each undulator beamline of the SHINE, the photon energy coverage with different operating beam energies is presented in Figure 2. There are two hard X-ray FEL beamlines, FEL-I and FEL-III.

The FEL-I is designed to cover the photon energy range of 3–15 keV. The baseline FEL operation modes are SASE and self-seeding with horizontal polarization, in which the normal planar undulator with a 26 mm undulator period, 1.05 T maximum magnetic peak field, and a 4 m segment length will be used. The output FEL photon is approximately $1 \times 10^{10} - 5 \times 10^{11}$ per pulse with a pulse duration of ~ 30 fs (FWHM) and up to a 1 MHz repetition rate and will be delivered to the end-stations, including the Hard X-ray Scattering and Spectroscopy End-station (HSS), the Coherent Diffraction End-station for Single Molecules and Particles (CDS), and the Station of Extreme Light (SEL).

The FEL-III is designed to cover the photon energy range of 10–25 keV, in which the superconducting planar undulator (vertical) with a 16 mm undulator period, 1.583 T maximum magnetic peak field, and a 4 m segment length is the first option. The baseline FEL modes of the FEL-III are SASE and hard X-ray self-seeding. It is a challenging task to develop a 4 m-length superconducting undulator with a maximum 1.583 T magnetic peak field. Hence, the alternative scheme design of the FEL-III that adopts an in-vacuum undulator with a 16 mm period length (IVU16) is also on standby to support FEL performance with a maximum 1.25 T magnetic peak field. The output FEL photon is approximately $2 \times 10^9 - 8 \times 10^{10}$ with a pulse duration of ~ 30 fs (FWHM) and a repetition rate of up to 0.1 MHz, and will be delivered to the end-stations, including the Hard X-ray Spectroscopy End-station (HXS), the Serial Femtosecond Crystallography End-station (SFX), the Coherent Diffraction Imaging-Imaging End-station for Materials (CDE-IEM), and the High Energy Density physics end-station (HED).

The FEL-II is the beamline that delivers the softest radiation of all FEL beamlines and is designed to cover the photon energy range from 0.4 to 3 keV. Actually, if required by scientific users, FEL radiation with photon energy as low as 0.08 keV is also achievable. The output radiation will be delivered to the downstream four serial experimental stations, namely, the Soft X-ray Scattering and Spectroscopy end-station (SSS), the Coherent Diffraction imaging End-station-Imaging End-station for Biomaterials (CDE-IEB), the Atomic, Molecular and Optical science end-station (AMO), and the Spectrometer for Electronic Structure end-station (SES). For the scientific objectives of the four end-stations, they aspire to cover the photon energy range from 0.2 to 3 keV, with a pulse energy of 10–300 μ J, pulse duration of less than 50 fs, and a maximum repetition rate of ≥ 100 kHz. The SES hopes to cover photon energy as low as 0.1 keV for the Angle Resolved PhotoEmission Spectroscopy experiment (ARPES). The AMO and IEB have higher expectations for the single-shot pulse energy and IEB and SES even hope for fully coherent radiation and circularly polarized radiation.

The FEL-II is the most diversified FEL beamline of the three FEL beamlines and includes SASE, self-seeding, EEHG, polarization control, and several more advanced FEL modes. It is worth mentioning that some of the advanced FEL modes have been commissioned and demonstrated at the Shanghai soft X-ray Free-Electron Laser facility (SXFEL), including HGHG, EEHG, HGHG-HGHG cascading, EEHG-HGHG cascading, harmonic lasing, polarization control, and fast-switch [14, 15, 30, 38]. Furthermore, the soft X-ray monochromator for self-seeding has been also arranged at the SXFEL and online for further testing. Given the arrangement of the whole project, the FEL-II will be the first undulator beamline which will start beam transportation and FEL commissioning in the spring of 2025.

2 Baseline design of the FEL-II

The design of the FEL-II undulator beamline aims to realize and exceed the regular SASE FEL operation to offer a fully coherent FEL pulse and several novel modes of operation for scientific users such as ultra-short pulse, polarization control, and fast switch. The baseline FEL operation modes consist of SASE, self-seeding, external seeding, and polarization control. In order to match these, a unique feature of this beamline is that it selects several kinds of undulator types, including main radiation undulator, modulation undulator, dual-period undulator, and elliptically polarized undulator (EPU). Considering the complexity and flexibility, the undulator module has been optimized to improve the performance of the baselines and several advanced FEL modes, and the layout is shown in Figure 3. The period length of the main radiator is 55 mm with 32 modules and a module length of 4 m, of which the first 14 modules are dual-period undulators with a switchable period of 75 mm (abbr. U55 and U75/55). The modulator period in the front of the beamline is 180 mm, which satisfies the FEL resonant condition with an approximately 260 nm seed laser at the electron beam energy range of 5–8 GeV. The EPU period is 55 mm (EPU55) with the plan of the Apple-X type, which is located downstream of the main radiators U55s as an afterburner for polarization control. There are five chicanes inserted, of which the first three are used for EEHG operation in the modulator section and the last two are used for self-seeding operation. Beyond the baseline design above, harmonic lasing, fresh bunch, ultra-short pulse, and polarization fast switch are also under construction.

2.1 SASE

The standard SASE configuration is the most general and popular FEL mode and has been adopted widely in the world. We present the following numerical simulation results using a Gaussian beam with the nominal beam parameter, a single SASE pulse spectrum in the time domain, and a frequency domain evaluated with a representative 1.24 keV photon energy, i.e., the 1.0 nm wavelength in Figure 4. The saturation peak power is nearly 10 GW and the pulse energy is nearly 300 μ J. The pulse length is about 28 fs (FWHM), and the radiation bandwidth is 0.31% (FWHM). It corresponds to a time-bandwidth product of 260, which is 600 times larger than that of the transform-limit pulse

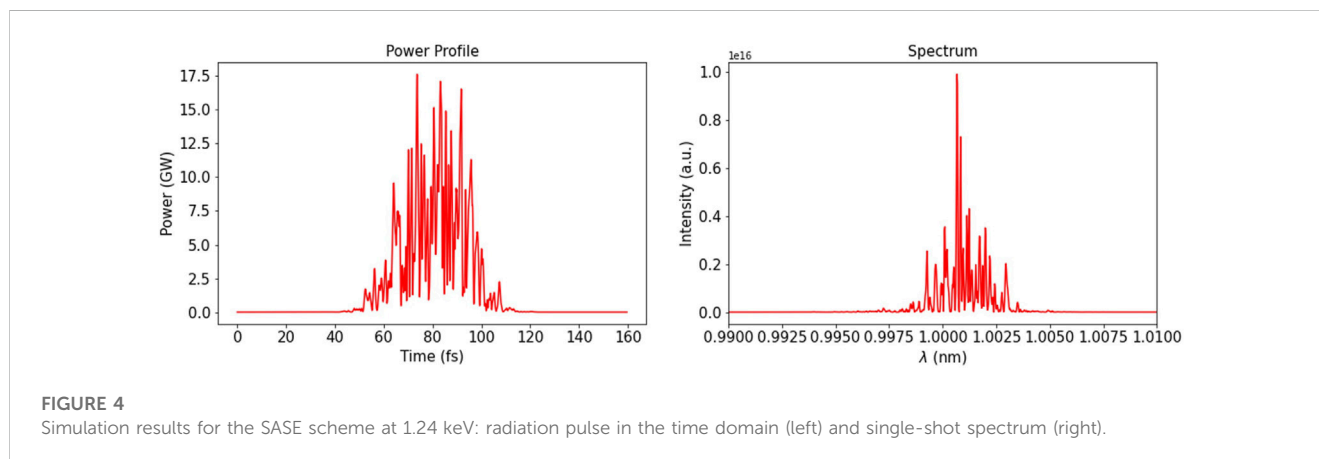
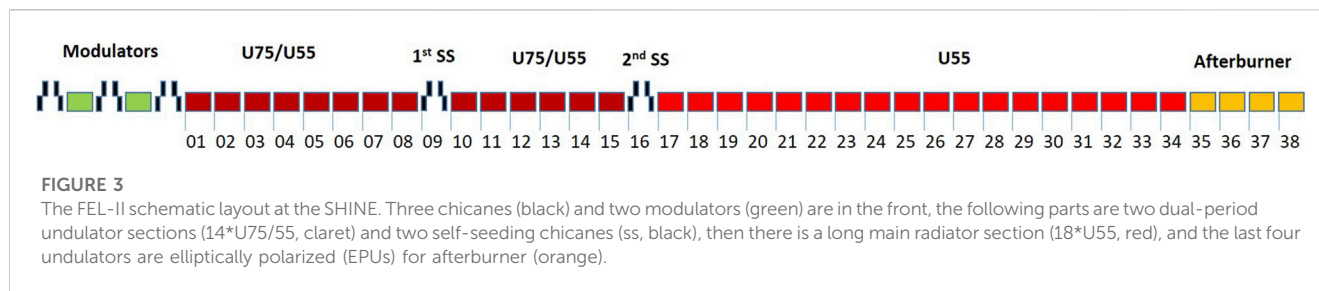


TABLE 1 SASE FEL performance of different photon energies in the FEL-II.

Specifications	Values						
Photon energy (keV)	0.4	0.6	0.9	1.24	2	2.5	3
Peak power (GW)	12.5	11.2	13.0	9.6	8.8	7.6	6.0
Pulse length (fs)	25	29	27	28	27	25	26
Bandwidth (% FWHM)	0.39	0.41	0.35	0.31	0.24	0.23	0.22
Pulse energy (μ J)	371	412	349	274	203	129	76
Source size (μ m, FWHM)	109	94	83	75	65	61	59
Divergence (μ rad, FWHM)	27.8	20.0	14.3	11.2	7.4	6.3	6.0

with a Gaussian profile. The FEL spot size near the saturation point is $75 \mu\text{m}$ (FWHM) and the divergence angle is $11 \mu\text{rad}$ (FWHM), which means the transverse coherence of the M2 factor is 1.9. Meanwhile, we can calculate that the FEL pulse contains 2.5×10^{12} photons, corresponding to the peak brightness of 8.9×10^{31} (photons/s/mm²/mrad²/0.1%BW) and the average brightness of 2.2×10^{24} (photons/s/mm²/mrad²/0.1%BW) at 1 MHz repetition rate. The undulator tapering technique application after FEL saturation can significantly improve the FEL power and pulse energy further [39]. For the FEL-II, the undulator module quantity is enough for the undulator tapering, therefore pulse energy larger than $500 \mu\text{J}$ and even to the 1 mJ level is possible for 1.24 keV. To illustrate the performance in the SASE mode, the

FEL properties in the SASE mode for 0.4 keV, 0.6 keV, 0.9 keV, 2.0 keV, 2.5 keV, and 3.0 keV photon energies are also given, as shown in Table 1. It is worth mentioning that, in order to increase the delivery and acceptance efficiency downstream for the lower photon energy radiation, e.g., 0.4 keV, FEL pulse optimization with a smaller divergence would be a more valuable objective.

2.2 Self-seeding

The X-ray radiation based on the SASE configuration is coherent spatially but lacks temporal coherence. The temporal and spectrum profiles exhibit a relatively wide bandwidth at the 0.1% level and a multi-spike structure characteristic of the SASE process due to the initial shot noise in the electron beam. The temporal coherence of SASE can be improved with the seeding technique that generates a narrow bandwidth pulse that is nearly Fourier transform-limited. External seeding and self-seeding technologies are configured in the FEL-II, which are used to cover the different photon energies. The self-seeding mode of the FEL-II is designed with a photon energy range of 0.6–1.5 keV and output spectral bandwidth of less than 0.02%. The layout of the soft X-ray self-seeding scheme (SXSS) is shown in Figure 5, which includes a two-stage self-seeding for sideband elimination, heat loading reduction, and high repetition rate operation.

Figure 6 illustrates the simulated self-seeding performances of 1.24 keV using a Gaussian beam. The saturation peak power is up to 15 GW with $390 \mu\text{J}$ pulse energy. The spectrum bandwidth equals to 0.024% (FWHM), and the temporal duration is approximately 50 fs

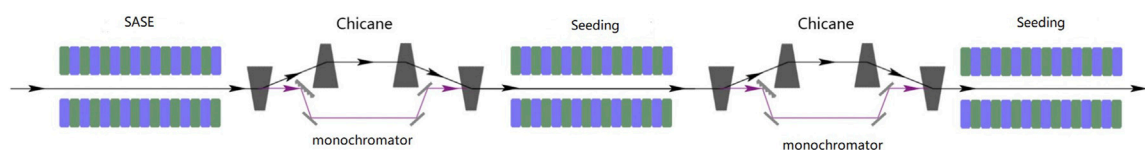


FIGURE 5

Soft X-ray self-seeding schematic design for the FEL-II. The two-stage self-seeding scheme is presented here. The two same self-seeding systems including an electron by-pass chicane and photon monochromator are inserted in the undulator beamline and separate 32 main radiators into three sections, i.e., the SASE section, and the 1st and 2nd seeding sections.

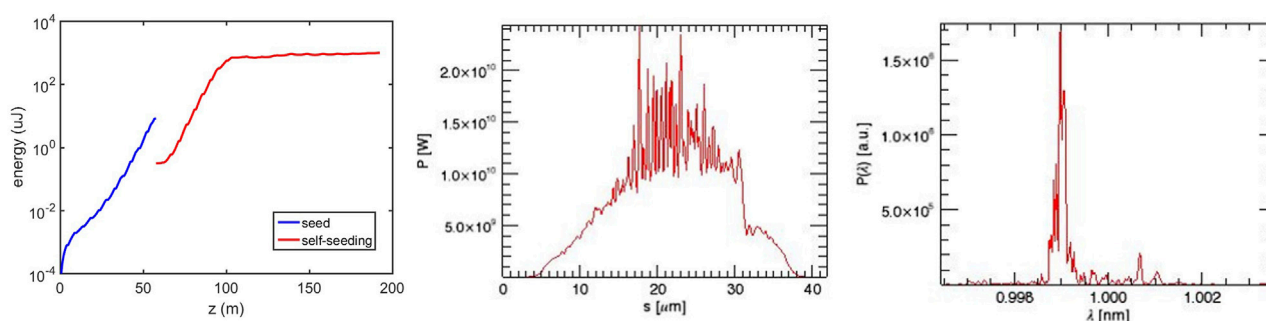


FIGURE 6

Simulation results for the SXSS scheme at 1.24 keV: the SXSS FEL pulse energy growth along the undulators beamline (left), output FEL pulse in the time domain (middle), and single-shot spectrum (right).

(FWHM), which gives a time-bandwidth product of 3.6, approximately 8 times larger than that of the transform-limited pulse with a Gaussian profile. The typical spot size and diffraction angle of the X-ray source are approximately $100 \mu\text{m}$ (FWHM) and $5.5 \mu\text{rad}$ (FWHM), respectively. With all the numbers, one can calculate that, the peak brilliance of FEL-II transmission-based self-seeding is 1.9×10^{33} (photons/s/mm²/mrad²/0.1%BW), at the photon energy of 1.24 keV. In order to suppress the side effect and mitigate the heat-loading on the grating, the two-stage SXSS mode can be operated.

For the SXSS mode with the grating-based photon monochromator, the SXSS system combined with a chicane is inserted in the undulator section with a 4 m length. The system includes two mirror boxes located at the two wings of the chicane and uses the configuration of LCLS as a reference [32, 40]. The front spectral box located between the first two dipoles of the chicane, consists of a cylindrical VLS grating and a plane mirror. The incidence of the VLS grating is fixed at 89° . The central wavelength adjustment depends on the off-axis rotation of the plane mirror. The rear mirror box located between the last two dipoles of the chicane consists of two cylindrical mirrors for the radiation spot focusing and radially optical path returning. The system is quite compact with a 4 m length, and the maximum delay time is approximately 1.5 ps, which is a challenge for mechanical design.

As mentioned above, the resolution is expected to be larger than 5,000 at the range of 0.6–1.5 keV, and we adopt a blazed grating and an alternative holographic grating, covering the different photon

energy, respectively. In order to further understand self-seeding, research and development has carried out on the monochromator system. At the end of 2022, the front box of the monochromator system based on the blazed grating has been installed at the beamline of the SXFEL facility and tested online. The test result presented a resolution larger than 5,300 at 520 eV. More detailed and systematic research is still ongoing.

2.3 EEHG

Besides the self-seeding technique, the external seeding technique is also employed in the FEL-II. The FEL radiation performances based on the external seeding technique, for example, temporal coherence, stability, and wavelength, are usually determined by the UV seed laser. Single-stage HGHG and EEHG are two basic operation modes. Different from the HGHG with relatively low harmonic up-conversion, the EEHG allows the up-conversion to higher harmonics and is capable of achieving higher than 50th harmonics. Theoretically, the 90th harmonics and even higher than 100th harmonics are possible to be produced, but it is difficult to achieve this experimentally due to the electron beam collective effects such as coherent synchrotron radiation (CSR), incoherent synchrotron radiation (ISR), and intra beam scattering (IBS). At the SXFEL facility, the 47th EEHG harmonic lasing has been demonstrated and passed the national acceptance, and the 54th harmonic lasing and the 61st harmonic signal have also been achieved during the commissioning. Thus, the

TABLE 2 Designed EEHG main parameters of the FEL-II.

Parameter	Value	Unit
Modulator period length	180	mm
Modulator total length	2.16	m
Seed laser wavelength	240–266	nm
Seed laser pulse duration (FWHM)	150	fs
Seed laser repetition rate	≥10	kHz
Seed laser pulse energy (rms)	≥400	μJ
Seed laser spot size (FWHM)	0.2	mm

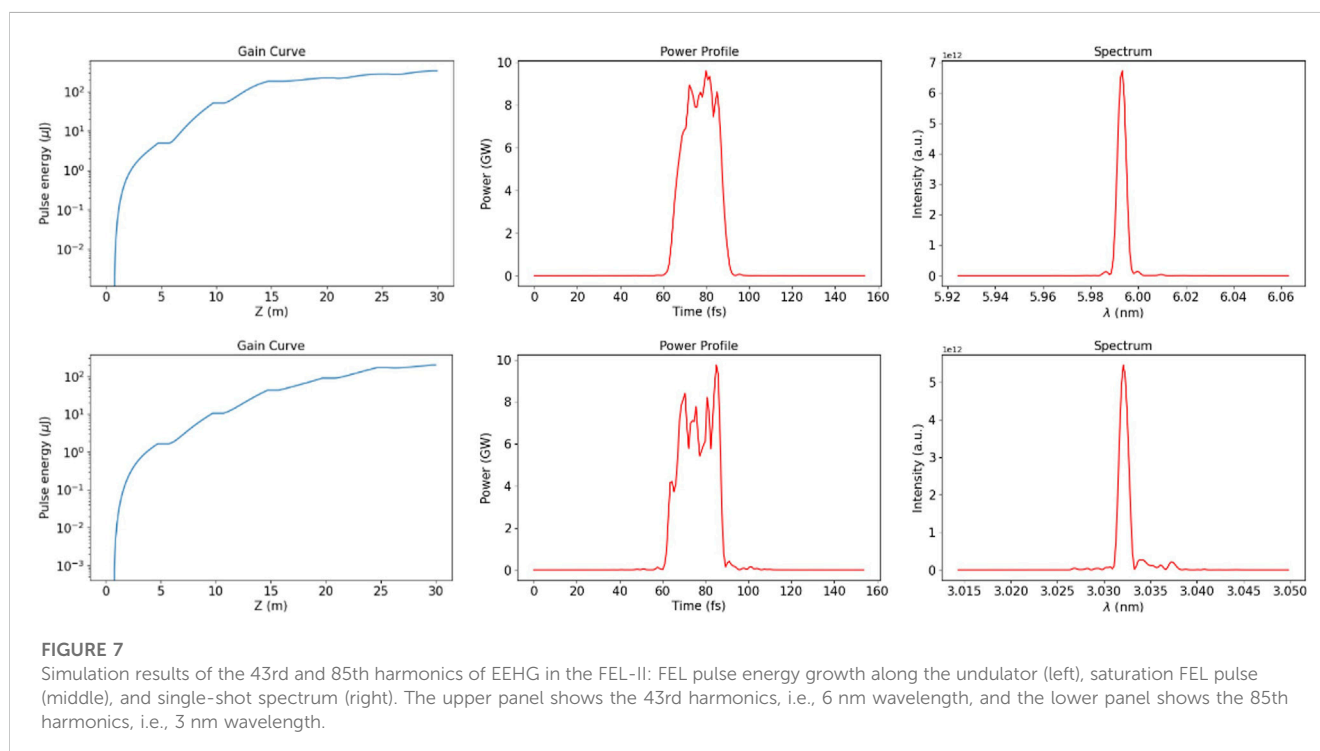
baseline design for the EEHG mode at the FEL-II is to generate fully coherent radiation at the photon energy up to 0.25 keV (5.0 nm, 54th harmonic), and the realization of 0.4 keV (3 nm, 90th harmonics) is still desirable in the future.

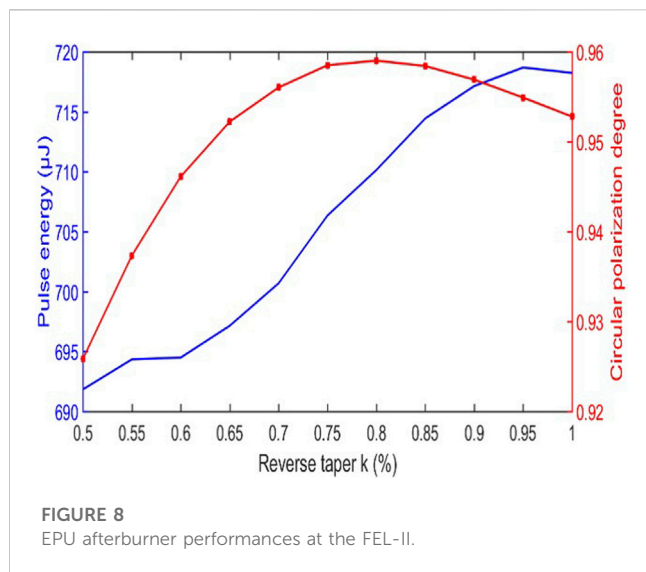
The modulator and the UV seed laser parameters of the FEL-II for the EEHG design and simulation are listed in Table 2. The seed laser is able to induce an energy modulation in beam longitudinal phase space with a maximum of 8 times the modulation amplitude of the beam slice energy spread, which basically satisfies the HGHG and EEHG operation requirements. The modulator has 12 periods with a total length of 2.16 m, which is optimized as approximately 3 times the FEL gain length of the 266 nm radiation. The 10 fs slippage length within the modulator ensures that the fresh-slice-based EEHG-HGHG cascading configuration depending on an ultra-short seed laser is possible for operation in the future.

Using a Gaussian beam, Figure 7 illustrates the performances of the 6 nm and 3 nm outputs at the FEL-II for the EEHG mode with

the harmonic number of 43 and 85, respectively. The EEHG-43 results show that a radiation peak power of up to 9.6 GW can be reached with a pulse energy larger than 180 μJ. The pulse duration is approximately 20 fs (FWHM), and the spectrum is quite narrow with a single spike and bandwidth of 0.065% (FWHM), corresponding to a time-bandwidth product of approximately 0.64, which is about 1.5 times larger than that of the transform-limit pulse with a Gaussian profile. In addition, the EEHG-85 results show that the radiation power can reach 9.8 GW and the pulse energy is approximately 170 μJ. The pulse duration is approximately 20 fs (FWHM), and the relative spectral bandwidth is 0.033% (FWHM), corresponding to a time-bandwidth product of about 0.65. It is worth noting that the micro-bunching instability contributed by the beam collective effects degrades the output performances partly, which has been analyzed before, but not presented here [41, 42].

The radiation undulator used for the EEHG operation is mainly the dual-period undulator U75/U55. As shown in Figure 2, the relatively lower harmonics operation depends on U75 with lower beam energy and while U55 is mainly used for the higher harmonics. It is worth noting that the EEHG source point is much earlier than the other FEL operation modes inevitably. For the beamline and end station, increasing the acceptance and tolerance of the optical design has to be taken into consideration. We also tried to enlarge the electron beam size in the undulator to reduce the radiation divergence. Simultaneously, the undulator taper technique which is usually used to increase the FEL pulse energy, will be used to stretch the spot waist longitudinally. In order to improve the delivery efficiency further due to the optical diffraction, the aperture of the vacuum pipe and the undulator gap are expanded and limited to larger than the FEL-I design. In addition, the injection and extraction of the seed laser is also a challenging task that is still ongoing. Up to now, we have optimized the lattice and shortened the





distance from laser injection to extraction further facing the challenge.

2.4 Afterburner

The main undulators adopt the plane-type undulator technique since it is more mature in terms of short periods, high magnetic field strength, and magnetic field error control. This is a benefit for FEL gain and reduces the cost of the device. However, the plane-type undulator provides a fixed polarization state which limits the user community. In order to obtain circularly polarized FEL radiation, a cross-plane undulator or an elliptically polarized undulator (EPU) might be the representative options. Consequently, we plan to install several EPU undulators in the form of afterburners downstream of the plane-type undulator section, so that the pre-clustered beam can emit near-saturated FEL radiation through the EPU undulators.

Polarized radiation based on EPU with a 55 mm undulator period length is designed to cover the same range of the SASE in the FEL-II with adjustable polarization. In order to ensure a relatively large photon energy range and flexibility, the advanced Apple-X type is taken into consideration. Figure 8 illustrates the polarization switch performances of 1.24 keV output, in which the reverse-taper technique is adopted. The reverse taper undulators are optimized to get maximum FEL power and high helicity purity. The maximum circular polarization is achieved with a reverse taper value of 0.8%, where the pulse energy is 720 μJ with about 96% degree of polarization.

3 Advanced FEL operation modes

In the previous section, the baseline configurations of the FEL-II undulator beamline, including SASE, self-seeding, EEHG, and polarization control were presented. However, our design work foresees physical and technical solutions which will allow significant performance enhancements without significant

changes to the infrastructure and hardware. Several potentials such as ultra-short, coherent X-ray coverage expansion, multi-color, polarization fast-switch, high-power FEL, and high-brightness SASE are under consideration for the future. It is worth noting that different FEL operation modes will require different beam properties, therefore, more flexibility of the schematic design at the FEL-II is still under consideration to allow further development.

3.1 Ultra-short pulse

Besides the baseline configuration of X-ray pulses with several tens of fs pulse duration, the users also require femtosecond level (even to attosecond) X-ray pulses for time-resolved studies of atomic and molecular processes. According to current progress in normal conducting FELs, the main feasible methods for ultra-short pulse generation are low charge mode, emittance spoiler foil, dechirper, and enhanced SASE (ESASE) technique [43–48].

The method of low charge mode has been extensively applied in many FEL facilities. Due to relaxed space charge effects, the electron beam can be compressed to the fs level in low charge mode. For the SHINE, the operation modes based on the 10 pC beam and 20 pC beam have been taken into consideration. FEL simulations show that the FEL pulse with a pulse duration of less than 10 fs and peak power at the GW level is feasible. The second method uses an emittance spoiler in the second bunch compressor. It is worth stressing that the thermal loading of the spoiler foil determines the maximum operational repetition rate. The third method uses a dechirper in the front of the undulator, where transverse wake and longitudinal wake would induce the fresh slices and change the pulse length for lasing. Further, multi-time slice slippages by utilizing the small chicane in-between undulators would improve the FEL peak power to 10–100 GW-level after saturation. In addition, the ESASE technique could also compress the bunch length to the fs level. ESASE employs an ultra-short infrared laser pulse to manipulate the beam's longitudinal phase space and imprint a very strong current enhancement on a small fraction of the electron beam. At the SHINE, with a currently available laser of 15 fs (FWHM) duration, 1.6 μm central wavelength, and 100 GW peak power, the peak current of the electron beam can be enhanced by approximately 7 times. These current spikes will generate ultra-short radiation pulses with a pulse duration of approximately 200 as and a peak power of about 70 GW in a 50 m long undulator in simulation. When using a shorter laser pulse with a 3 fs (FWHM) pulse duration, we can get a single spike X-ray pulse from the ESASE. The peak power exceeds 30 GW after a 40 m long undulator. The longitudinal coherence has also been improved due to the short pulse duration. The ultra-short ESASE radiation pulse is naturally locked to the optical laser, thus allowing a pump-probe experiment to be performed with high temporal resolution.

3.2 Harmonic lasing

The SHINE is constructed to cover the photon energy from 0.4 keV to 25 keV based on SASE mode, which is also capable to be

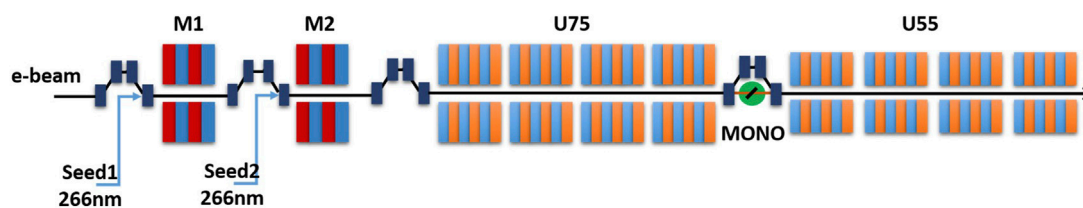


FIGURE 9

Advanced FEL configurations for coherent X-ray full coverage at the FEL-II. It mainly consists of the EEHG section (two seed lasers, two modulators, and three chicanes), U75 section, self-seeding section, and U55 section.

less than 0.4 keV for the requirements of scientific research. However, the energy range of the fully coherent FEL modes is less than the SASE mode. It should be noted that there are two energy gaps that can not be covered, one of which is the approximate 1.5–4.5 keV range between SXSS and HXSS modes, and another one is the approximate 0.25–0.6 keV range between EEHG and SXSS modes. Several advanced FEL configurations can be attempted in the FEL-II beamline and are promising to cover the energy gaps. The higher harmonics up-conversion to 90th of the single-stage EEHG is relatively difficult to realize.

However, due to the configuration of the different undulator periods, harmonic lasing is a better way to expand the coherent X-ray coverage range. Usually, harmonic lasing is used for SASE-dependent harmonic lasing schemes based on two different undulator periods [49–51]. In order to expand the coherent X-ray coverage range, EEHG harmonic cascading can be operated at 0.25–0.6 keV, and self-seeding harmonic lasing can cover 1.5–4.5 keV [52]. Consequently, the full coverage of the coherent X-ray FEL can be expected due to the flexible infrastructure.

As shown in Figure 2, for the 5 GeV operation, the single stage EEHG with the 75 mm-period undulator easily generates the FEL output with a wavelength of 5–10 nm (≤ 0.25 keV), and the 2–3rd harmonic lasing with the 55 mm-period undulator is expected to cover the wavelength of 2–5 nm, i.e., 0.25–0.6 keV. For the SXSS harmonic lasing, the pure 55 mm-period undulator covers the coherent hard X-ray photon energy gap. Figure 2 tells us that the 55 mm-period undulator can cover photon energy of 0.54–6.0 keV for the 8 GeV operation. Therefore, the undulators upstream are used for the SXSS operation and generate the FEL output with a photon energy of 0.54–1.5 keV, and the 2–3rd harmonic lasing with the undulator downstream can cover the photon energy of 1.5–4.5 keV. In the simulation, we have seen a quasi-coherent X-ray generation within the two energy gaps connecting with the reverse taper technique, and the current setup has already offered the requirement of the harmonic lasing schemes.

3.3 EEHG-HGHG cascading

For the external seeding technique of the FEL-II at the SHINE, the baseline design is the EEHG operation with the highest harmonics of approximately 50. For the FEL simulation, higher harmonics are possible based on single-stage EEHG or EEHG-HGHG cascading. At the SXFEL facility, the EEHG-HGHG

cascading scheme has been demonstrated experimentally [38]. For the single-stage EEHG, the 54th harmonics, i.e., 5nm, has been demonstrated and the higher harmonics commissioning is ongoing. Therefore, to cover the photon energy between 0.25 and 0.6 keV, and meet the needs of users, the advanced EEHG-HGHG cascading mode is an option with the fresh bunch technique. Figure 9 presents the current schematic layout which only requires a minor improvement for the EEHG-HGHG cascading operation. The first-stage EEHG will generate the FEL pulse with a 3–9 nm wavelength in U75s, which is the seed of the second-stage HGHG to generate the FEL pulse with a 1–3 nm wavelength in U55s. Figure 10 presents the EEHG-HGHG cascading simulation results, where the wavelength of the first-stage EEHG is 3 nm as a harmonic up-conversion of approximately 90 and the second-stage HGHG is 1 nm as a harmonic up-conversion of 3. The final output peak power of the 1 nm wavelength X-ray pulse is approximately 8 GW and the pulse energy is more than 100 μ J with a spectrum close to Fourier-transform-limited. For this scheme, a flat-top distribution of the current profile for the electron beam is required. The key point is an fs level time jitter which impacts the stability of the output FEL power significantly [42].

3.4 Multi-color

In the past few years, several techniques for multi-color operation and spectral control of X-ray FELs have been developed worldwide. The key to achieving multi-color pulse generation is easily understood from the basic principles of FEL operation. The multi-color experiment usually employs de-chirpers, chicanes, and, of course, the central wavelengths of the FEL pulses can be independently tuned by simply changing the gaps of the undulator [53–62]. All the components will be established at the facility, thus it is very convenient for delivering multi-color and/or multi-pulse to the experimental stations. Because of the long undulator, one can display the powerful ability of multi-color operation at the SHINE.

3.5 HB-SASE

The high-brightness SASE (HB-SASE) technique can be applied to significantly improve the temporal coherence of SASE [63]. By inserting a series of small chicanes between the undulator segments of SASE, the slippage length between the FEL

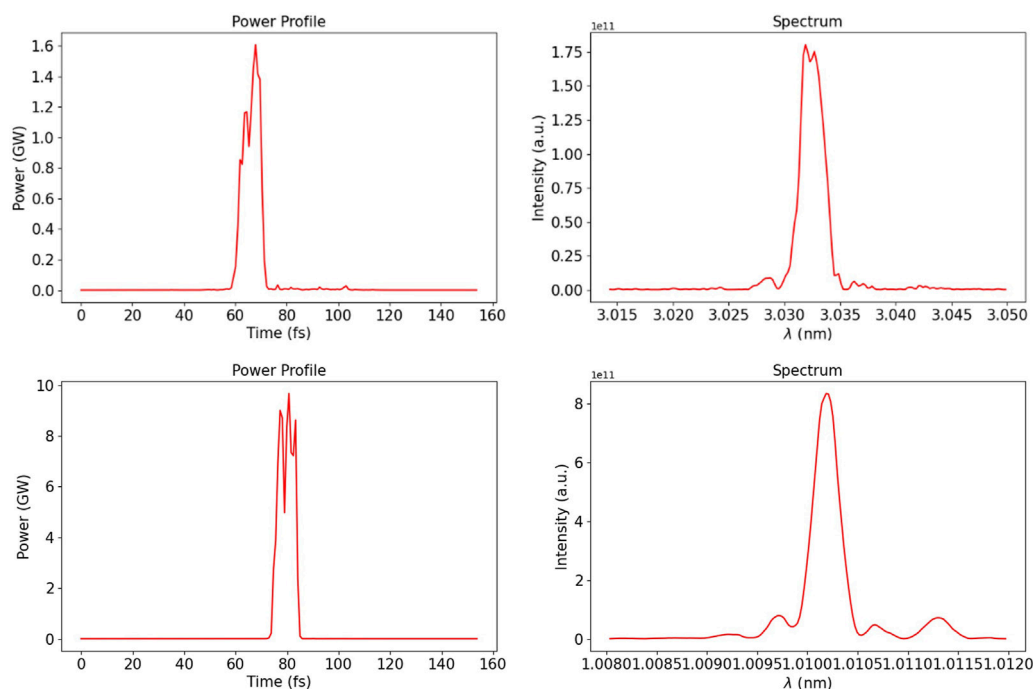


FIGURE 10

EEHG-HGHG cascading simulation results. The top two are the first-stage 90th EEHG with 3 nm wavelength and the bottom two are the second-stage 3rd HGHG with 1 nm wavelength.

radiation and electron bunch can be artificially increased, giving a corresponding increase in coherence length and a narrowing output bandwidth. The HB-SASE technique does not require an external seeding source or X-ray photon optics and is applicable at any wavelength and repetition rate. In the SHINE design, the length of each undulator module is 5 m, and a delay sequence based on prime number increases is used. The delay induced by the first small chicane is approximately 36 nm, which is a little longer than the slippage length in one undulator module. The simulation shows that the peak power of the HB-SASE is comparable with the normal SASE. The longitudinal phase distribution of the HB-SASE is smoother, which results in a much narrower bandwidth of approximately 0.003%, approximately 20 times narrower than that of the normal SASE case.

3.6 Others

There are still several other advanced FEL operation modes on the way one of which is a high-power SASE a high-power SASE scheme. The basic method adopts the dechirper to kick the beam slice and generate multi-stage slippage between the beam slice and the FEL pulse, which could increase the FEL peak power to several times the saturation power. We are also working on the polarization fast-switch based on a fast-switch phase shifter. The fast-switch phase shifter with a length of less than 3 m and a 0.5 MHz switch frequency will be inserted between the four EPU undulators to continuously switch between the different polarization states.

Simulation results show that two different polarization FEL pulses with higher than 90% polarization degree are theoretically achievable.

4 Summary

In summary, this article presents the physical design of the FEL-II undulator beamline at the SHINE, which is the first high repetition rate based hard X-ray FEL facility in China. The SHINE completed an international review of the physical design at the end of 2022, and this work in detail is presented first as a manuscript. We mainly introduce the FEL-II, which is the most diversified undulator beamline compared to the FEL-I and the FEL-III.

The baseline design mainly consisting of SASE, self-seeding, external seeding, and polarization control, will provide X-ray FEL pulses beyond the photon energy range from 0.4 to 3.0 keV with a repetition rate up to 1 MHz. Furthermore, the FEL-II is also designed to provide more flexible FEL output properties towards ultra-short pulse, coherent X-ray coverage expansion, multi-color, and so on. This beamline aims to be one of the most advanced FEL beamlines in the world and meet the needs of more scientific users. As the softest X-ray beamline of the SHINE, the commissioning and operation of the FEL-II beamline will be started firstly, and the comprehensive advance in engineering construction is urgent and important in the coming years. The research and development program, including the prototype construction of the undulator, the magnet device, and the

beam measurement device, will be completed in 2023. After this, effective serial production and installation may start by 2024. After the installation, the FEL commissioning of the FEL-II beamline will start, and realize the first lasing by June 2025.

Author contributions

All authors contributed to the article and approved the submitted version. The first author TL wrote most of the manuscript and contributed to the physical design of all FEL schemes. NH, HY, and ZG contributed to the different scheme designs and simulations. ZQ, KZ, SC, CF, WZ, HaL, XF, HeL, and BF partially contributed to the scheme design, simulation, test, and manuscript writing. The corresponding authors HD and BL took the head in the accelerator and FEL scheme design, reviewed the manuscript, and supervised the work. DW and ZZ were in charge of the whole project design and construction.

Funding

This work was partially supported by the National Natural Science Foundation of China (11905277, 12125508, 11935020, 11975300 and 12122514), the CAS Project for Young Scientists in Basic Research (YSBR60 and YSBR42), Youth Innovation Promotion Association CAS (2023302), Program of Shanghai

Academic/Technology Research Leader (21XD1404100), Natural Science Foundation of Shanghai (23ZR1471300), and Shanghai Pilot Program for Basic Research—Chinese Academy of Science, Shanghai Branch (JCYJ-SHFY-2021-010).

Acknowledgments

The authors would like to thank the whole FEL team in SARI for their excellent contributions to the FEL-II physical design and preparation at the SHINE.

Conflict of interest

The authors declare that the research was conducted in the absence of any commercial or financial relationships that could be construed as a potential conflict of interest.

Publisher's note

All claims expressed in this article are solely those of the authors and do not necessarily represent those of their affiliated organizations, or those of the publisher, the editors and the reviewers. Any product that may be evaluated in this article, or claim that may be made by its manufacturer, is not guaranteed or endorsed by the publisher.

References

1. Madey JM. Stimulated emission of bremsstrahlung in a periodic magnetic field. *J Appl Phys* (1971) 42:1906–13. doi:10.1063/1.1660466
2. Huang Z, Kim K-J. Review of x-ray free-electron laser theory. *Phys Rev ST Accel Beams* (2007) 10:034801. doi:10.1103/PhysRevSTAB.10.034801
3. Huang N, Deng H, Liu B, Wang D, Zhao Z. Features and futures of x-ray free-electron lasers. *The Innovation* (2021) 2. doi:10.1016/j.xinn.2021.100097
4. Bostedt C, Boutet S, Fritz DM, Huang Z, Lee HJ, Lemke HT, et al. Linac coherent light source: The first five years. *Rev Mod Phys* (2016) 88:015007. doi:10.1103/RevModPhys.88.015007
5. Young L, Kanter EP, Krässig B, Li Y, March AM, Pratt ST, et al. Femtosecond electronic response of atoms to ultra-intense x-rays. *Nature* (2010) 466:56–61. doi:10.1038/nature09177
6. Chapman HN. Femtosecond x-ray protein nanocrystallography. *Nature* (2010) 470:73–7. doi:10.1038/nature09750
7. Ackermann W, Asova G, Ayvazyan V, Azima A, Baboi N, Bähr J, et al. Operation of a free-electron laser from the extreme ultraviolet to the water window. *Nat Photon* (2007) 1:336–42. doi:10.1038/nphoton.2007.76
8. Emma P, Akre R, Arthur J, Bionta R, Bostedt C, Bozek J, et al. First lasing and operation of an ångström-wavelength free-electron laser. *Nat Photon* (2010) 4:641–7. doi:10.1038/nphoton.2010.176
9. Ishikawa T, Aoyagi H, Asaka T, Asano Y, Azumi N, Bizen T, et al. A compact x-ray free-electron laser emitting in the sub-ångström region. *Nat Photon* (2012) 6:540–4. doi:10.1038/nphoton.2012.141
10. Allaria E, Appio R, Badano L, Barletta WA, Bassanese S, Biedron SG, et al. Highly coherent and stable pulses from the fermi seeded free-electron laser in the extreme ultraviolet. *Nat Photon* (2012) 6:699–704. doi:10.1038/nphoton.2012.233
11. Kang H-S, Min C-K, Heo H, Kim C, Yang H, Kim G, et al. Hard x-ray free-electron laser with femtosecond-scale timing jitter. *Nat Photon* (2017) 11:708–13. doi:10.1038/s41566-017-0029-8
12. Decking W, Abeghyan A, Abramian P, Abramsky A, Aguirre A, Albrecht C, et al. A mhz-repetition-rate hard x-ray free-electron laser driven by a superconducting linear accelerator. *Nat Photon* (2020) 14:391–7. doi:10.1038/s41566-020-0607-z
13. Prat E, Abela R, Aiba M, Alarcon A, Alex J, Arbelo Y, et al. A compact and cost-effective hard x-ray free-electron laser driven by a high-brightness and low-energy electron beam. *Nat Photon* (2020) 14:748–54. doi:10.1038/s41566-020-00712-8
14. Zhao Z, Wang D, Gu Q, andMing Gu LY, Leng Y, Liu B. Status of the sxfel facility. *Appl Sci* (2017) 7:607. doi:10.3390/app7060607
15. Liu B, Zhang W, Fang W, Wang Z, Zhou Q, Leng Y, et al. The sxfel upgrade: From test facility to user facility. *Appl Sci* (2021) 12:176. doi:10.3390/app12010176
16. Kondratenko A, Saldin E. Generation of coherent radiation by a beam of relativistic electrons in an undulator. *Sov Phys - Tech Phys (Engl Transl.); (United States)* (1981) 26:8.
17. Bonifacio R, Pellegrini C, Narducci L. Collective instabilities and high-gain regime in a free electron laser. *Opt Commun* (1984) 50:373–8. doi:10.1016/0030-4018(84)90105-6
18. Yu LH. Generation of intense uv radiation by subharmonically seeded single-pass free-electron lasers. *Phys Rev A* (1991) 44:5178–93. doi:10.1103/PhysRevA.44.5178
19. Yu L-H, Babzien M, Ben-Zvi I, DiMauro LF, Doyuran A, Graves W, et al. High-gain harmonic-generation free-electron laser. *Science* (2000) 289:932–4. doi:10.1126/science.289.5481.932
20. Stupakov G. Using the beam-echo effect for generation of short-wavelength radiation. *Phys Rev Lett* (2009) 102:074801. doi:10.1103/PhysRevLett.102.074801
21. Xiang D, Stupakov G. Echo-enabled harmonic generation free electron laser. *Phys Rev ST Accel Beams* (2009) 12:030702. doi:10.1103/PhysRevSTAB.12.030702
22. Geloni G, Kocharyan V, Saldin E. A novel self-seeding scheme for hard x-ray fels. *J Mod Opt* (2011) 58:1391–403. doi:10.1080/09500340.2011.586473
23. Amann J, Berg W, Blank V, Decker F-J, Ding Y, Emma P, et al. Demonstration of self-seeding in a hard-x-ray free-electron laser. *Nat Photon* (2012) 6:693–8. doi:10.1038/nphoton.2012.180
24. Liu B, Li WB, Chen JH, Chen ZH, Deng HX, Ding JG, et al. Demonstration of a widely-tunable and fully-coherent high-gain harmonic-generation free-electron laser. *Phys Rev ST Accel Beams* (2013) 16:020704. doi:10.1103/PhysRevSTAB.16.020704
25. Xiang D, Colby E, Dunning M, Gilevich S, Hast C, Jobe K, et al. Demonstration of the echo-enabled harmonic generation technique for short-wavelength seeded free electron lasers. *Phys Rev Lett* (2010) 105:114801. doi:10.1103/PhysRevLett.105.114801

26. Xiang D, Colby E, Dunning M, Gilevich S, Hast C, Jobe K, et al. Evidence of high harmonics from echo-enabled harmonic generation for seeding x-ray free electron lasers. *Phys Rev Lett* (2012) 108:024802. doi:10.1103/PhysRevLett.108.024802
27. Hemsing E, Dunning M, Garcia B, Hast C, Raubenheimer T, Stupakov G, et al. Echo-enabled harmonics up to the 75th order from precisely tailored electron beams. *Nat Photon* (2016) 10:512–5. doi:10.1038/nphoton.2016.101
28. Zhao ZT, Wang D, Chen JH, Chen ZH, Deng HX, Ding JG, et al. First lasing of an echo-enabled harmonic generation free-electron laser. *Nat Photon* (2012) 6:360–3. doi:10.1038/nphoton.2012.105
29. Ribic PR, Abrami A, Badano L, Bossi M, Braun H-H, Bruchon N, et al. Coherent soft x-ray pulses from an echo-enabled harmonic generation free-electron laser. *Nat Photon* (2019) 13:555–61. doi:10.1038/s41566-019-0427-1
30. Feng C, Deng H, Zhang M, Wang X, Chen S, Liu T, et al. Coherent extreme ultraviolet free-electron laser with echo-enabled harmonic generation. *Phys Rev Accel Beams* (2019) 22:050703. doi:10.1103/PhysRevAccelBeams.22.050703
31. Feldhaus J, Saldin E, Schneider J, Schneidmiller E, Yurkov M. Possible application of x-ray optical elements for reducing the spectral bandwidth of an x-ray sase fel. *Opt Commun* (1997) 140:341–52. doi:10.1016/S0030-4018(97)00163-6
32. Ratner D, Abela R, Amann J, Behrens C, Bohler D, Bouchard G, et al. Experimental demonstration of a soft x-ray self-seeded free-electron laser. *Phys Rev Lett* (2015) 114. doi:10.1103/PhysRevLett.114.054801
33. Nam I, Min C-K, Oh B, Kim G, Na D, Suh YJ, et al. High-brightness self-seeded x-ray free-electron laser covering the 3.5keV to 14.6keV range. *Nat Photon* (2021) 10:435–41. doi:10.1038/s41566-021-00777-z
34. Liu S, Decking W, Kocharyan V, Saldin E, Serkez S, Shayduk R, et al. Preparing for high-repetition rate hard x-ray self-seeding at the European x-ray free electron laser: Challenges and opportunities. *Phys Rev Accel Beams* (2019) 22:060704. doi:10.1103/PhysRevAccelBeams.22.060704
35. Inoue I, Osaka T, Hara T, Tanaka T, Inagaki T, Fukui T, et al. Generation of narrow-band x-ray free-electron laser via reflection self-seeding. *Nat Photon* (2019) 13:319–22. doi:10.1038/s41566-019-0365-y
36. Huang N-S, Liu Z-P, Deng B-J, Zhu Z-H, Li S-H, Liu T, et al. The ming proposal at shine: Megahertz cavity enhanced x-ray generation. *Nucl Sci Tech* (2023) 34:2210–3147. doi:10.1007/s41365-022-01151-6
37. Zhao Z, Wang D, Yang Z, Yin L. Sclf: An 8-gev cw scrflinac-based x-ray fel facility in shanghai. *Int Free Electron Laser Conf* (2018) 2018. doi:10.18429/JACoW-FEL2017-MOP055
38. Feng C, Liu T, Chen S, Zhou K, Zhang K, Qi Z, et al. Coherent and ultrashort soft x-ray pulses from echo-enabled harmonic cascade free-electron lasers. *Optica* (2022) 9:785–91. doi:10.1364/OPTICA.466064
39. Kroll N, Morton P, Rosenbluth M. Free-electron lasers with variable parameter wigglers. *IEEE J Quan Elect* (1981) 17:1436–68. doi:10.1109/JQE.1981.1071285
40. Cocco D, Abela R, Amann J, Chow K, Emma P, Feng Y, et al. The optical design of the soft x-ray self seeding at lcls. *Proc SPIE* (2013) 8849. doi:10.1117/12.2024402
41. Zhou K, Feng C, Wang D. Feasibility study of generating ultra-high harmonic radiation with a single stage echo-enabled harmonic generation scheme. *Nucl Instr Methods Phys Res Section A: Acc Spectrometers, Detectors Associated Equipment* (2016) 834:30–5. doi:10.1016/j.nima.2016.07.021
42. Yang H, Yan J, Zhu Z, Deng H. Optimization and stability analysis of the cascaded eehg-hghg free-electron laser. *Nucl Instr Methods Phys Res Section A: Acc Spectrometers, Detectors Associated Equipment* (2022) 1039:167065. doi:10.1016/j.nima.2022.167065
43. Reiche S, Musumeci P, Pellegrini C, Rosenzweig J. Development of ultra-short pulse, single coherent spike for sase x-ray fels. *Nucl Instr Methods Phys Res Section A: Acc Spectrometers, Detectors Associated Equipment* (2008) 593:45–8. doi:10.1016/j.nima.2008.04.061
44. Ding Y, Brachmann A, Decker F-J, Dowell D, Emma P, Frisch J, et al. Measurements and simulations of ultralow emittance and ultrashort electron beams in the linac coherent light source. *Phys Rev Lett* (2009) 102:254801. doi:10.1103/PhysRevLett.102.254801
45. Emma P, Bane K, Cornacchia M, Huang Z, Schlarb H, Stupakov G, et al. Femtosecond and subfemtosecond x-ray pulses from a self-amplified spontaneous-emission-based free-electron laser. *Phys Rev Lett* (2004) 92:074801. doi:10.1103/PhysRevLett.92.074801
46. Ding Y, Behrens C, Coffee R, Decker F-J, Emma P, Field C, et al. Generating femtosecond x-ray pulses using an emittance-spoiling foil in free-electron lasers. *Appl Phys Lett* (2015) 107:191104. doi:10.1063/1.4935429
47. Zholotov AA. Method of an enhanced self-amplified spontaneous emission for x-ray free electron lasers. *Phys Rev ST Accel Beams* (2005) 8:040701. doi:10.1103/PhysRevSTAB.8.040701
48. Duris J, Li S, Driver T, Champenois EG, MacArthur JP, Lutman AA, et al. Tunable isolated attosecond x-ray pulses with gigawatt peak power from a free-electron laser. *Nat Photon* (2019) 14. doi:10.1038/s41566-019-0549-5
49. Schneidmiller EA, Yurkov MV. Harmonic lasing in x-ray free electron lasers. *Phys Rev ST Accel Beams* (2012) 15:080702. doi:10.1103/PhysRevSTAB.15.080702
50. Schneidmiller EA, Faatz B, Kuhlmann M, Rönsch-Schulenburg J, Schreiber S, Tischer M, et al. First operation of a harmonic lasing self-seeded free electron laser. *Phys Rev Accel Beams* (2017) 20:020705. doi:10.1103/PhysRevAccelBeams.20.020705
51. Prat E, Reiche S. Compact coherence enhancement by subharmonic self-seeding in X-ray free-electron laser facilities. *J Synchrotron Radiat* (2018) 25:329–35. doi:10.1107/S1600577518000395
52. Zhang K, Qi Z, Feng C, Deng H, Wang D, Zhao Z. Extending the photon energy coverage of an x-ray self-seeding fel via the reverse taper enhanced harmonic generation technique. *Nucl Instr Methods Phys Res Section A: Acc Spectrometers, Detectors Associated Equipment* (2017) 854:3–10. doi:10.1016/j.nima.2017.02.039
53. Ciocci F, Dattoli G, Pagnutti S, Petralia A, Sabia E, Ottaviani PL, et al. Two color free-electron laser and frequency beating. *Phys Rev Lett* (2013) 111:264801. doi:10.1103/PhysRevLett.111.264801
54. Lutman AA, Coffee R, Ding Y, Huang Z, Krzywinski J, Maxwell T, et al. Experimental demonstration of femtosecond two-color x-ray free-electron lasers. *Phys Rev Lett* (2013) 110:134801. doi:10.1103/PhysRevLett.110.134801
55. Hara T, Inubushi Y, Katayama T, Sato T, Tanaka H, Tanaka T, et al. Two-colour hard x-ray free-electron laser with wide tunability. *Nat Commun* (2013) 4:2919. doi:10.1038/ncomms3919
56. Lutman AA, Maxwell TJ, MacArthur JP, Guetg MW, Berrah N, Coffee RN, et al. Fresh-slice multicolour x-ray free-electron lasers. *Nat Photon* (2016) 10:745–50. doi:10.1038/nphoton.2016.201
57. Guetg MW, Lutman AA, Ding Y, Maxwell TJ, Huang Z. Dispersion-based fresh-slice scheme for free-electron lasers. *Phys Rev Lett* (2018) 120:264802. doi:10.1103/PhysRevLett.120.264802
58. Reiche S, Prat E. Two-color operation of a free-electron laser with a tilted beam. *J Synchrotron Radiat* (2016) 23:869–73. doi:10.1107/S1600577516007189
59. Dijkstal P, Malyzhenkov A, Reiche S, Prat E. Demonstration of two-color x-ray free-electron laser pulses with a sextupole magnet. *Phys Rev Accel Beams* (2020) 23:030703. doi:10.1103/PhysRevAccelBeams.23.030703
60. Qin W, Ding Y, Lutman AA, Chao Y-C. Matching-based fresh-slice method for generating two-color x-ray free-electron lasers. *Phys Rev Accel Beams* (2017) 20:090701. doi:10.1103/PhysRevAccelBeams.20.090701
61. Chao Y-C, Qin W, Ding Y, Lutman AA, Maxwell T. Control of the lasing slice by transverse mismatch in an x-ray free-electron laser. *Phys Rev Lett* (2018) 121:064802. doi:10.1103/PhysRevLett.121.064802
62. Feng C, Deng H. Multicolour emission. *Nat Photon* (2016) 10:695–6. doi:10.1038/nphoton.2016.204
63. McNeil BWJ, Thompson NR, Dunning DJ. Transform-limited x-ray pulse generation from a high-brightness self-amplified spontaneous-emission free-electron laser. *Phys Rev Lett* (2013) 110:134802. doi:10.1103/PhysRevLett.110.134802